

Deformation in transversely isotropic thermoelastic medium using new modified couple stress theory in frequency domain

Parveen Lata^a and Harpreet Kaur*

Department of Basic and Applied Sciences, Punjabi University, Patiala, Punjab, India

(Received July 5, 2019, Revised October 9, 2019, Accepted November 11, 2019)

Abstract. The objective of this paper is to study the two dimensional deformation in transversely isotropic thermoelastic medium without energy dissipation due to time harmonic sources using new modified couple stress theory, a continuum theory capable to predict the size effects at micro/nano scale. The couple stress constitutive relationships have been introduced for transversely isotropic thermoelastic medium, in which the curvature tensor is asymmetric and the couple stress moment tensor is symmetric. Fourier transform technique is applied to obtain the solutions of the governing equations. Assuming the deformation to be harmonically time-dependent, the transformed solution is obtained in the frequency domain. The application of a time harmonic concentrated and distributed sources have been considered to show the utility of the solution obtained. The displacement components, stress components, temperature change and couple stress are obtained in the transformed domain. A numerical inversion technique has been used to obtain the solutions in the physical domain. The effects of angular frequency are depicted graphically on the resulted quantities.

Keywords: new modified couple stress theory; length scale parameters; transversely isotropic; concentrated and distributed sources; harmonic behavior; Fourier transform; angular frequency

1. Introduction

Couple stress theory is an extension to continuum theory that includes the effects of couple stresses, in addition to the classical direct and shear forces per unit area. First mathematical model to examine the materials with couple stresses was presented by Cosserat and Cosserat (1909). In this theory, both curvature tensor and the couple stress moment tensor are asymmetric and every particle is assumed to be capable of both linear displacement and rotation during the deformation of the material. Because of the failure of establishing the constitutive relationships, this theory was not given importance by researchers. However, Tiwari (1971) determined the effect of couple stress on deflection produced in a semi-infinite elastic body because of impulsive twist over surface using Cosserat equations. Mindlin and Tierstein (1962) and Koiter (1964) developed initial version of couple stress theory, based on the Cosserat continuum theory (1909). Koiter (1964) introduced the constitutive relationships for couple stress theory, involving length scale parameters to predict the size effects. These lengths are a material property on which effect of couple stresses depends strongly and can be find out by means of test. This theory suffers from some inconsistencies, such as the indeterminacy of the couple-stress tensor, inconsistent boundary conditions and the consideration of the redundant

body couple distribution. A modified couple stress theory (M-CST) with one length scale parameter was presented by Yang *et al.* (2002) using the balance law for moments of couple besides the balance laws for forces and moment of forces. Application of this equilibrium equation leads to a symmetric couple-stress tensor. M-CST cannot describe the pure bending of plate properly as no couple stresses and no size-effects are predicted for pure bending of plate. So, Hadjesfandiari *et al.* (2011) presented consistent couple stress theory (C-CST) with the skew-symmetric couple-stresses, which resolves all the discrepancies of modified couple stress theory. Laminated composite materials are anisotropic and are generally used in engineering. Modified couple stress theory was not applicable to anisotropic materials. So, Chen and Li (2014) presented the new modified couple stress theory (NM-CST) for anisotropic materials containing three length scale parameters. For NM-couple stress theory,

$$\begin{aligned}\chi_{ij} &= \omega_{i,j}, \\ \omega_i &= \frac{1}{2} e_{ijk} u_{k,j}, \\ \sigma_{ij} &= c_{ijkl} \varepsilon_{kl}, \\ m_{ij} &= l_i^2 G_i \chi_{ij} + l_j^2 G_j \chi_{ji}, \\ \varepsilon_{ij} &= \frac{1}{2} (u_{i,j} + u_{j,i}),\end{aligned}$$

Here, u_i is the displacement vector, m_{ij} is couple stress moment tensor, σ_{ij} is stress tensor, ε_{ij} is strain tensor, χ_{ij} is curvature tensor, ω_i are rotation components, c_{ijkl} are elastic parameters, l_i and l_j are material length scale

*Corresponding author, Ph.D. Scholar
E-mail: mehrokpreet93@gmail.com

^aAssociate Professor
E-mail: parveenlata@pbi.ac.in

parameters.

Ke *et al.* (2012) studied the nonlinear free vibration problem of a functionally graded micro-beam according to the modified couple stress theory. Najafi (2012) investigated the quality factor of thermo-elastic damping in an electro-statically deflected micro-beam resonator using Hamilton principles based on modified couple stress theory and hyperbolic heat conduction model. Kang *et al.* (2012) studied the static deformation behavior of a piezoelectric micromachined ultrasonic transducer (PMUT) actuated by a strong external electric field. The optimal ratio of the top electrode diameter and the membrane diameter is found to around 0.674 and this value is independent of any other parameters if the thicknesses of the two electrodes are negligible as compared to those of piezoelectric and passive layers. Free vibration analysis of a three dimensional cylindrical micro-beam on the basis of modified couple stress theory was done by Wang *et al.* (2013). Reddy *et al.* (2013) examined the bending of simply supported micro isotropic plates using modified couple stress theory and a meshless method. The added scale parameter produced an effect according to the size of the plate, the effect getting to be smaller as the plate size is increased. Yingly *et al.* (2013) analyzed a thermally and electrically actuated functionally graded material (FGM) microbeam using modified couple stress theory, considering Casimir and van der Waals forces. They determined the effect of the various factors on the pull-in voltage of the microbeam and deduce that non-uniform thermal actuation is more effective than uniform thermal actuation in actuating FGM cantilever. Shaat *et al.* (2014) studied the bending analysis of nano-sized Kirchhoff plates using modified couple-stress theory including surface energy and microstructure effects. Chen *et al.* (2014) studied the scale effects of composite laminated plates using new modified couple stress theory by finite element method. Thai *et al.* (2014) studied the Static bending, buckling and free vibration behaviors of size-dependent functionally graded (FG) sandwich microbeams based on the modified couple stress theory and Timoshenko beam theory and using closed form solutions. It was deduced that inclusion of the small scale effect makes the beam stiffer, and thus leads to a reduction of both stress and deflection and an increase in the natural frequency and critical buckling load. Ansari *et al.* (2014) presented an exact solution for the vibration analysis of piezoelectric microbeams on the basis of the modified couple stress theory for both Euler-Bernoulli and Timoshenko beam models using Hamilton's principle. It was shown that when the length of microbeams is decreased, effects of piezoelectricity and size effects are more prominent. Kumar and Devi (2015) studied the influence of Hall current and rotation in thermoelastic diffusive media caused by ramp type loading on the basis of modified couple stress theory using Laplace and Fourier Transform techniques. Atanasov *et al.* (2017) examined the thermal effect on the free vibration and buckling of the Euler-Bernoulli double microbeam system based on the modified couple stress theory using Bernoulli-Fourier method. Togun and Bağdatlı (2017) presented the linear free vibration of a simply-supported nanobeam by using modified couple stress theory

and Hamilton's principle. Also, they analyzed the effects of the length scale parameter and the Poisson's ratio on natural frequency showing that the natural frequency is decreased as the dimensionless scale parameter is magnified. Vibrational frequency of a tapered microbeam resonator was examined via a generalized thermoelastic theory and modified couple stress theory by Zenkour (2018). Hadesfandiari *et al.* (2018) developed size-dependent Timoshenko beam model using C-CST. Kaushal *et al.* (2010) discussed response of frequency domain in generalized thermoelasticity with two temperatures. Kumar *et al.* (2017) studied the Rayleigh waves in anisotropic magneto-thermoelastic medium with two temperature, in the presence of Hall current and rotation. The two-dimensional problem of expanding ring load in a modified couple stress theory of thermoelastic diffusion with heat sources in time and frequency domains with one and two relaxation times using Laplace and Hankel transforms is investigated by Kumar *et al.* (2017). Abbas *et al.* (2009,2014a) studied different problems under two-temperature generalized thermoelastic theory by finite element method. Abbas *et al.* (2014,2015) studied phase lag models in fiber-reinforced anisotropic materials using generalized thermoelasticity. Jahangir *et al.* (2013,2015) studied the magneto-thermo-microstretch elastic solid under the effect of gravity with energy dissipation using generalized theory of thermoelasticity. Despite of this several researchers worked on different theory of thermoelasticity as Marin (1997,2007), Marin and Stan (2013), Marin (1998), Jahangir *et al.* (2018, 2018a,2018b), Lata *et al.* (2016,2016a,2017a) Lata and Kaur (2019,2019a,2019b), Abbas *et al.* (2012,2016,2014b,2014c).

In the present investigation, our objective is to study the deformation in transversely isotropic thermoelastic medium using new modified couple stress theory without energy dissipation in frequency domain. The medium is subjected to the thermal and mechanical sources. In the constitutive relationships the curvature (rotation gradient) tensor is asymmetric and the couple stress moment tensor is symmetric. Deformation is assumed to be harmonically time-dependent. Fourier transform technique is applied to obtain the solutions of the governing equations. The displacement components, stress components, temperature change and couple stress are obtained in the transformed domain and are presented graphically for different values of distance. The effects of angular frequency on resulting quantities are also depicted graphically.

2. Basic equations

Following Chen and Li (2014) and Kumar and Devi (2015), the field equations transversely isotropic thermoelastic medium using new modified couple stress theory in the absence of body forces, body couple and without energy dissipation are given by

$$\sigma_{ij} = c_{ijkl}\varepsilon_{kl} + \frac{1}{2}e_{ijk}m_{lk,l} - \beta_{ij}T, \quad (1)$$

$$c_{ijkl}\varepsilon_{kl,j} + \frac{1}{2}e_{ijk}m_{lk,lj} - \beta_{ij}T_{,j} = \rho\ddot{u}_i, \quad (2)$$

$$K_{ij}T_{,ij} - \rho C_E \ddot{T} = \beta_{ij} T_0 \ddot{\epsilon}_{ij}, \quad (3)$$

where

$$\beta_{ij} = c_{ijkl} \alpha_{ij}, \quad (4)$$

$$\epsilon_{ij} = \frac{1}{2} (u_{i,j} + u_{j,i}), \quad (5)$$

$$m_{ij} = l_i^2 G_i \chi_{ij} + l_j^2 G_j \chi_{ji}, \quad (6)$$

$$\chi_{ij} = \omega_{i,j}, \quad (7)$$

$$\omega_i = \frac{1}{2} e_{ijk} u_{k,j}. \quad (8)$$

Here, $u = (u_1, u_2, u_3)$ is the components of displacement vector, c_{ijkl} ($c_{ijkl} = c_{ijlk} = c_{jikl} = c_{jilk}$) are elastic parameters, σ_{ij} are the components of stress tensor, ϵ_{ij} are the components of strain tensor, e_{ijk} is alternate tensor, m_{ij} are the components of couple-stress, α_{ij} are the coefficients of linear thermal expansion, β_{ij} is thermal tensor, T is the temperature change, l_i ($i = 1, 2, 3$) are material length scale parameters, χ_{ij} is curvature, ω_i is the rotational vector, ρ is the density, K_{ij} is the materialistic constant, C_E is the specific heat at constant strain, T_0 is the reference temperature assumed to be such that $T/T_0 \ll 1$, G_i are the elasticity constants and $\beta_1 = (c_{11} + c_{12})\alpha_1 + c_{13}\alpha_3$, $\beta_3 = 2c_{13}\alpha_1 + c_{33}\alpha_3$.

3. Formulation and solution of the problem

We consider a two dimensional transversely isotropic thermoelastic homogeneous medium using new modified couple stress theory initially at uniform temperature T_0 occupying the region of a half space $x_3 \geq 0$. A rectangular coordinate system (x_1, x_2, x_3) having origin on the surface $x_3 = 0$ has been taken. All the field quantities depend on (x_1, x_3, t) . We have used appropriate transformation using Slaughter (2002), on the set of equation (1)-(3) to derive the equations for transversely isotropic thermoelastic solid under consideration.

Equations of motion in $u_1 - u_3$ plane are given by

$$c_{11}u_{1,11} + \left(c_{44} + \frac{1}{4}l_2^2 G_2 \nabla^2\right)u_{1,33} + \left(c_{13} + c_{44} - \frac{1}{4}l_2^2 G_2 \nabla^2\right)u_{3,13} - \beta_1 \frac{\partial T}{\partial x_1} = \rho \ddot{u}_1, \quad (9)$$

$$c_{33}u_{3,33} + \left(c_{44} + c_{13} - \frac{1}{4}l_2^2 G_2 \nabla^2\right)u_{1,31} + \left(c_{44} + \frac{1}{4}l_2^2 G_2 \nabla^2\right)u_{3,11} - \beta_3 \frac{\partial T}{\partial x_3} = \rho \ddot{u}_3, \quad (10)$$

Equation of heat conduction without energy dissipation is given by

$$K_1 \frac{\partial^2 T}{\partial x_1^2} + K_3 \frac{\partial^2 T}{\partial x_3^2} - \rho C_E \frac{\partial^2 T}{\partial t^2} = T_0 \frac{\partial}{\partial t} \left(\beta_1 \frac{\partial u_1}{\partial x_1} + \beta_3 \frac{\partial u_3}{\partial x_3} \right), \quad (11)$$

where

$$\beta_1 = (c_{11} + c_{12})\alpha_1 + c_{13}\alpha_3, \quad \beta_3 = 2c_{13}\alpha_1 + c_{33}\alpha_3.$$

where comma in the subscript denotes the derivative w.r.t. distance component written after comma. In the above equation we use contracting subscript notation ($1 \rightarrow 11, 2 \rightarrow 22, 3 \rightarrow 33, 4 \rightarrow 23, 5 \rightarrow 31, 6 \rightarrow 12$) to relate c_{ijkl} to c_{mn} .

And the constitutive relationships are

$$\sigma_{33} = c_{13} \frac{\partial u_1}{\partial x_1} + c_{33} \frac{\partial u_3}{\partial x_3} - \beta_3 T, \quad (12)$$

$$\sigma_{33} = c_{13} \frac{\partial u_1}{\partial x_1} + c_{33} \frac{\partial u_3}{\partial x_3} - \beta_3 T, \quad (13)$$

$$m_{32} = \frac{1}{2} (l_2^2 G_2 - l_3^2 G_3) \left(\frac{\partial^2 u_1}{\partial x_3^2} - \frac{\partial^2 u_3}{\partial x_1 \partial x_3} \right). \quad (14)$$

To facilitate the solution following dimensionless quantities are used

$$x'_1 = \frac{x_1}{L}, \quad x'_3 = \frac{x_3}{L}, \quad u'_1 = \frac{\rho c_1^2}{L \beta_1 T_0} u_1, \quad u'_3 = \frac{\rho c_1^2}{L \beta_1 T_0} u_3, \quad T' = \frac{T}{T_0}, \quad t' = \frac{c_1}{L} t, \quad \sigma'_{11} = \frac{\sigma_{11}}{\beta_1 T_0}, \quad \sigma'_{33} = \frac{\sigma_{33}}{\beta_1 T_0}, \quad m'_{32} = \frac{m_{32}}{L \beta_1 T_0}, \quad (15)$$

where $c_1^2 = \frac{c_{11}}{\rho}$ and L is constant of dimension of length.

Using the dimensionless quantities defined by (15) into Eqs. (9)-(14) and suppressing the primes, we obtain

$$\frac{\partial^2 u_1}{\partial x_1^2} + \left(\delta_1 + \frac{1}{4L^2 c_{11}} l_2^2 G_2 \left(\frac{\partial^2}{\partial x_1^2} + \frac{\partial^2}{\partial x_3^2} \right) \right) \frac{\partial^2 u_1}{\partial x_3^2} + \left(\delta_2 - \frac{1}{4L^2 c_{11}} l_2^2 G_2 \left(\frac{\partial^2}{\partial x_1^2} + \frac{\partial^2}{\partial x_3^2} \right) \right) \frac{\partial^2 u_3}{\partial x_1 \partial x_3} - \frac{\partial T}{\partial x_1} = \frac{\partial^2 u_1}{\partial t^2}, \quad (16)$$

$$\delta_4 \frac{\partial^2 u_3}{\partial x_3^2} + \left(\delta_2 - \frac{1}{4L^2 c_{11}} l_2^2 G_2 \left(\frac{\partial^2}{\partial x_1^2} + \frac{\partial^2}{\partial x_3^2} \right) \right) \frac{\partial^2 u_1}{\partial x_1 \partial x_3} + \left(\delta_1 - \frac{1}{4L^2 c_{11}} l_2^2 G_2 \left(\frac{\partial^2}{\partial x_1^2} + \frac{\partial^2}{\partial x_3^2} \right) \right) \frac{\partial^2 u_3}{\partial x_1^2} - p_5 \frac{\partial T}{\partial x_3} = \frac{\partial^2 u_3}{\partial t^2}, \quad (17)$$

$$c_1 \frac{\partial^2 T}{\partial x_1^2} + p_3 c_1 \frac{\partial^2 T}{\partial x_3^2} = \zeta_1 L \frac{\partial^2 u_1}{\partial t \partial x_1} + \zeta_2 L \frac{\partial^2 u_3}{\partial t \partial x_3} + \zeta_3 c_1 \frac{\partial^2 T}{\partial t^2}, \quad (18)$$

$$\sigma_{33} = \frac{c_{13}}{\rho c_1^2} \frac{\partial u_1}{\partial x_1} + \frac{c_{33}}{\rho c_1^2} \frac{\partial u_3}{\partial x_3} - p_5 T, \quad (19)$$

$$\sigma_{31} = \frac{c_{44}}{\rho c_1^2} \left(\frac{\partial u_1}{\partial x_3} + \frac{\partial u_3}{\partial x_1} \right) + \frac{1}{4\rho c_1^2 L^2} \left((l_1^2 G_1 - l_2^2 G_2) \left(-\frac{\partial^3 u_1}{\partial x_3 \partial x_1^2} + \frac{\partial^3 u_3}{\partial x_1^3} \right) + (l_3^2 G_3 - l_2^2 G_2) \left(-\frac{\partial^3 u_1}{\partial x_1 \partial x_3^2} + \frac{\partial^3 u_3}{\partial x_1^2 \partial x_3} \right) \right) \quad (20)$$

$$m_{32} = \frac{1}{2} \frac{\beta_1 T_0}{L^2 \rho c_1^2} (l_2^2 G_2 - l_3^2 G_3) \left(\frac{\partial^2 u_1}{\partial x_3^2} - \frac{\partial^2 u_3}{\partial x_1 \partial x_3} \right), \quad (21)$$

where

$$\delta_1 = \frac{c_{44}}{c_{11}}, \quad \delta_2 = \frac{c_{13} + c_{44}}{c_{11}}, \quad \delta_4 = \frac{c_{33}}{c_{11}}, \quad p_5 = \frac{\beta_3}{\beta_1}, \quad p_3 = \frac{K_3}{K_1}, \quad \zeta_1 = \frac{T_0 \beta_1^2}{K_1 \rho}, \quad \zeta_2 = \frac{T_0 \beta_1 \beta_3}{K_1 \rho}, \quad \zeta_3 = \frac{C_E c_{11}}{K_1}$$

The initial and regularity conditions are given by

$$\begin{aligned} u_1(x_1, x_3, 0) = 0 &= \dot{u}_1(x_1, x_3, 0), \\ u_3(x_1, x_3, 0) = 0 &= \dot{u}_3(x_1, x_3, 0), \\ T(x_1, x_3, 0) = 0 &= \dot{T}(x_1, x_3, 0) \text{ for } x_3 \geq 0, -\infty < x_1 < \infty \\ u_1(x_1, x_3, t) = u_3(x_1, x_3, t) = T(x_1, x_3, 0) = 0 &\text{ for } t > 0 \text{ when } x_3 \rightarrow \infty \end{aligned} \tag{22}$$

Assuming harmonic behaviour as

$$(u_1, u_3, T)(x_1, x_3, t) = (u_1, u_3, T)(x_1, x_3)e^{i\omega t}, \tag{23}$$

where ω is the angular frequency, the Eqs. (9)-(14) recast into

$$\begin{aligned} \frac{\partial^2 u_1}{\partial x_1^2} + \left(\delta_1 + \frac{1}{4L^2 c_{11}} l_2^2 G_2 \left(\frac{\partial^2}{\partial x_1^2} + \frac{\partial^2}{\partial x_3^2} \right) \right) \frac{\partial^2 u_1}{\partial x_3^2} + \left(\delta_2 - \frac{1}{4L^2 c_{11}} l_2^2 G_2 \left(\frac{\partial^2}{\partial x_1^2} + \frac{\partial^2}{\partial x_3^2} \right) \right) \frac{\partial^2 u_3}{\partial x_1 \partial x_3} - \frac{\partial T}{\partial x_1} = -\omega^2 u_1, \end{aligned} \tag{24}$$

$$\begin{aligned} \delta_4 \frac{\partial^2 u_3}{\partial x_3^2} + \left(\delta_2 - \frac{1}{4L^2 c_{11}} l_2^2 G_2 \left(\frac{\partial^2}{\partial x_1^2} + \frac{\partial^2}{\partial x_3^2} \right) \right) \frac{\partial^2 u_3}{\partial x_1 \partial x_3} + \left(\delta_1 + \frac{1}{4L^2 c_{11}} l_2^2 G_2 \left(\frac{\partial^2}{\partial x_1^2} + \frac{\partial^2}{\partial x_3^2} \right) \right) \frac{\partial^2 u_3}{\partial x_1^2} - p_5 \frac{\partial T}{\partial x_3} = -\omega^2 u_3, \end{aligned} \tag{25}$$

$$c_1 \frac{\partial^2 T}{\partial x_1^2} + p_3 c_1 \frac{\partial^2 T}{\partial x_3^2} = \zeta_1 Li\omega \frac{\partial u_1}{\partial x_1} + \zeta_2 Li\omega \frac{\partial u_3}{\partial x_3} - \omega^2 c_1 \zeta_3 T, \tag{26}$$

$$\sigma_{33} = \frac{c_{13}}{\rho c_1^2} \frac{\partial u_1}{\partial x_1} + \frac{c_{33}}{\rho c_1^2} \frac{\partial u_3}{\partial x_3} - p_5 T, \tag{27}$$

$$\begin{aligned} \sigma_{31} = \frac{c_{44}}{\rho c_1^2} \left(\frac{\partial u_1}{\partial x_3} + \frac{\partial u_3}{\partial x_1} \right) + \frac{1}{4\rho c_1^2 L^2} \left((l_1^2 G_1 - l_2^2 G_2) \left(-\frac{\partial^3 u_1}{\partial x_3 \partial x_1^2} + \frac{\partial^3 u_3}{\partial x_1^2} \right) + (l_3^2 G_3 - l_2^2 G_2) \left(-\frac{\partial^3 u_1}{\partial x_1 \partial x_3^2} + \frac{\partial^3 u_3}{\partial x_3^2} \right) \right), \end{aligned} \tag{28}$$

$$m_{32} = \frac{1}{2} \frac{\beta_1 T_0}{L^2 \rho c_1^2} (l_2^2 G_2 - l_3^2 G_3) \left(\frac{\partial^2 u_1}{\partial x_3^2} - \frac{\partial^2 u_3}{\partial x_1 \partial x_3} \right). \tag{29}$$

Defining the Fourier transformation as

$$\hat{f}(\xi, x_3, \omega) = \int_{-\infty}^{\infty} f(x_1, x_3, \omega) e^{i\xi x_1} dx_1. \tag{30}$$

Applying (30) to the equation (24)-(29), we obtain system of three homogeneous equations from equations (24)-(26). These resulting equations have non trivial solution if the determinant of the coefficient $(\hat{u}_1, \hat{u}_3, \hat{T})$ vanishes, which yields the following characteristic equation

$$\left(P \frac{d^8}{dx_3^8} + Q \frac{d^6}{dx_3^6} + R \frac{d^4}{dx_3^4} + S \frac{d^2}{dx_3^2} + T \right) (\hat{u}_1, \hat{u}_3, \hat{T}) = 0 \tag{31}$$

where

$$P = -p_3 c_1 \delta_4 \frac{l_2^2 G_2}{4L^2 c_{11}},$$

$$Q = i\zeta_2 \omega L p_5 \frac{l_2^2 G_2}{4L^2 c_{11}} - p_3 c_1 \left(\left(\delta_1 - \frac{l_2^2 G_2}{4L^2 c_{11}} \xi^2 \right) \delta_4 - \frac{l_2^2 G_2}{4L^2 c_{11}} \omega^2 + 2\xi^2 (\delta_1 + \delta_2) \frac{l_2^2 G_2}{4L^2 c_{11}} \right) - c_1 (\xi^2 - \zeta_3 \omega^2) \delta_4 \frac{l_2^2 G_2}{4L^2 c_{11}},$$

$$\begin{aligned} R = -\xi^2 \zeta_1 Li\omega \frac{p_5 l_2^2 G_2}{4L^2 c_{11}} - p_3 c_1 \left(\delta_4 (-\xi^2 + \omega^2) - \xi^2 \left(\delta_1^2 - \delta_2^2 - 2(\delta_1 + \delta_2) \frac{l_2^2 G_2}{4L^2 c_{11}} \xi^2 \right) - \xi^2 (-\xi^2 + \omega^2) \frac{l_2^2 G_2}{4L^2 c_{11}} + \left(\delta_1 - \frac{l_2^2 G_2}{4L^2 c_{11}} \xi^2 \right) (\omega^2) \right) + c_1 (\xi^2 - \omega^2 \zeta_3) \left(\left(\delta_1 - \frac{l_2^2 G_2}{4L^2 c_{11}} \xi^2 \right) \delta_4 + \frac{l_2^2 G_2}{4L^2 c_{11}} (\omega^2) \right) - 2\xi^2 (\delta_1 + \delta_2) \frac{l_2^2 G_2}{4L^2 c_{11}} + i\zeta_2 \omega L \left(p_5 \left(\delta_1 + \frac{l_2^2 G_2}{4L^2 c_{11}} \xi^2 \right) + \xi^2 \frac{l_2^2 G_2}{4L^2 c_{11}} \right), \end{aligned}$$

$$\begin{aligned} S = \xi^2 \zeta_1 Li\omega \left(p_5 \left(\delta_2 + \frac{l_2^2 G_2}{4L^2 c_{11}} \xi^2 \right) + \left(\delta_4 + \frac{l_2^2 G_2}{4L^2 c_{11}} \xi^2 \right) \right) - \zeta_2 i\omega L (-p_5 (-\xi^2 + \omega^2) - \xi^2 (\delta_2 + \frac{l_2^2 G_2}{4L^2 c_{11}} \xi^2)) + c_1 (\xi^2 - \omega^2 \zeta_3) \left(-\delta_4 (-\xi^2 + \omega^2) - \xi^2 (-\xi^2 - \omega^2) \frac{l_2^2 G_2}{4L^2 c_{11}} \right) + \left(\delta_1 + \frac{l_2^2 G_2}{4L^2 c_{11}} \xi^2 \right) (\omega^2) - \xi^2 \left(\delta_1^2 - \delta_2^2 - 2(\delta_1 + \delta_2) \frac{l_2^2 G_2}{4L^2 c_{11}} \xi^2 \right) - p_3 c_1 ((-\xi^2 + \omega^2) \omega^2 - (\xi^2 + \omega^2) \xi^2) \left(\delta_1 + \frac{l_2^2 G_2}{4L^2 c_{11}} \xi^2 \right), \end{aligned}$$

$$T = c_1 (\xi^2 - \omega^2 \zeta_3) \left((-\xi^2 + \omega^2) \omega^2 - \xi^2 (-\xi^2 + \omega^2) \left(\delta_1 - \frac{l_2^2 G_2}{4L^2 c_{11}} \xi^2 \right) \right) + \xi^2 \zeta_1 i\omega L (-\omega^2 + \xi^2).$$

The roots of the equation (31) are $\pm \lambda_i (i = 1, 2, 3, 4)$, using the radiation condition that $\hat{u}_1, \hat{u}_3, \hat{T} \rightarrow 0$ as $x_3 \rightarrow \infty$ the solution of equation (31) may be written as

$$\hat{u}_1 = A_1 e^{-\lambda_1 x_3} + A_2 e^{-\lambda_2 x_3} + A_3 e^{-\lambda_3 x_3} + A_4 e^{-\lambda_4 x_3}, \tag{32}$$

$$\begin{aligned} \hat{u}_3 = d_1 A_1 e^{-\lambda_1 x_3} + d_2 A_2 e^{-\lambda_2 x_3} + d_3 A_3 e^{-\lambda_3 x_3} + d_4 A_4 e^{-\lambda_4 x_3}, \end{aligned} \tag{33}$$

$$\begin{aligned} \hat{T} = g_1 A_1 e^{-\lambda_1 x_3} + g_2 A_2 e^{-\lambda_2 x_3} + g_3 A_3 e^{-\lambda_3 x_3} + g_4 A_4 e^{-\lambda_4 x_3}, \end{aligned} \tag{34}$$

where

$$\begin{aligned} d_i = \frac{\lambda_i^6 p_3 c_1 l_2^2 G_2 + \lambda_i^4 (-p_3 c_1 \epsilon_1 - c_1 (\xi^2 - \omega^2 \zeta_3) l_2^2 G_2) + \lambda_i^2 ((\xi^2 - \omega^2) p_3 c_1 + \epsilon_1 \epsilon_2) - (\xi^2 - \omega^2) \epsilon_2 - \xi^2 \zeta_1 Li\omega}{-\lambda_i^4 p_3 c_1 \epsilon_3 + \lambda_i^2 (-p_3 c_1 (-\omega^2 + \xi^2 \epsilon_1) + \epsilon_2 \epsilon_3 + \zeta_2 i\omega L p_5) - (-\omega^2 + \xi^2 \epsilon_1) \epsilon_2} \\ g_i = \frac{-\lambda_i^6 \delta_4 l_2^2 G_2 + \lambda_i^4 (\epsilon_1 \delta_4 - \omega^2 l_2^2 G_2 + 2\xi^2 (\delta_1 + \delta_2) l_2^2 G_2) + \lambda_i^2 ((-\xi^2 + \omega^2) \epsilon_3 - \epsilon_1 (-\omega^2 + \xi^2 \epsilon_1) + \xi^2 (\delta_2 - l_2^2 G_2 \xi^2)) + (-\xi^2 + \omega^2) (\omega^2 - \xi^2 \epsilon_1)}{-\lambda_i^4 p_3 c_1 \epsilon_3 + \lambda_i^2 ((-\omega^2 + \xi^2 \epsilon_1) p_3 c_1 + \epsilon_2 \epsilon_3 + \zeta_2 i\omega L p_5) - (-\omega^2 + \xi^2 \epsilon_1) \epsilon_2} \\ \epsilon_1 = (\delta_1 + l_2^2 G_2 \xi^2), \epsilon_2 = c_1 (\xi^2 - \omega^2 \zeta_3), \epsilon_3 = (\delta_4 + l_2^2 G_2 \xi^2). \end{aligned}$$

4. Boundary conditions

On the half-space surface ($x_3 = 0$) normal point force and thermal point source, which are assumed to be time harmonic, are applied. We consider two types of boundary conditions, as follows

Case 1: The normal/mechanical force on the surface of half-space

The boundary conditions in this case are

1. Condition of normal stress

$$\sigma_{33}(x_1, x_3, t) = -F_1 \psi_1(x) e^{i\omega t}, \tag{35}$$

2. Vanishing of tangential stress

$$\sigma_{31}(x_1, x_3, t) = 0, \tag{36}$$

3. Vanishing of tangential couple stress

$$m_{32}(x_1, x_3, t) = 0, \tag{37}$$

4. Condition of temperature change

$$\frac{\partial T}{\partial x_3}(x_1, x_3, t) = 0 \text{ at } x_3 = 0, \tag{38}$$

where F_1 is the magnitude of the force applied, $\psi_1(x)$ specify the source distribution function along x_1 axis.

Case 2: The thermal source on the surface of half-space
When the plane boundary is stress free and subjected to

thermal point source, the boundary conditions in this case are

$$\sigma_{31}(x_1, x_3, t) = 0, \tag{39}$$

$$\sigma_{31}(x_1, x_3, t) = 0, \tag{40}$$

$$m_{32}(x_1, x_3, t) = 0, \tag{41}$$

$$\frac{\partial T}{\partial x_3}(x_1, x_3, t) = F_2 \psi_1(x) e^{i\omega t} \text{ at } x_3 = 0, \tag{42}$$

where F_2 is the constant temperature applied on the boundary, $\psi_1(x)$ specify the source distribution function along x_1 axis.

Subcase 1(a). Mechanical force on the surface of half space

Substituting the values of $\widehat{u}_1, \widehat{u}_3, \widehat{T}$ from Eqs. (32)-(34) in the boundary conditions (35)-(38) and with the aid of (1), (5)-(8),(22)-(23),(27)-(30), we obtain the components of displacement, normal stress, tangential stress, tangential couple stress and temperature change as

$$\widehat{u}_1 = -\frac{F_1 \widehat{\psi}_1(\xi)}{\Delta} (B_{11} e^{-\lambda_1 x_3} + B_{12} e^{-\lambda_2 x_3} + B_{13} e^{-\lambda_3 x_3} + B_{14} e^{-\lambda_4 x_3}) e^{i\omega t}, \tag{43}$$

$$\widehat{u}_3 = -\frac{F_1 \widehat{\psi}_1(\xi)}{\Delta} (d_1 B_{11} e^{-\lambda_1 x_3} + d_2 B_{12} e^{-\lambda_2 x_3} + d_3 B_{13} e^{-\lambda_3 x_3} + d_4 B_{14} e^{-\lambda_4 x_3}) e^{i\omega t}, \tag{44}$$

$$\widehat{T} = -\frac{F_1 \widehat{\psi}_1(\xi)}{\Delta} (g_1 B_{11} e^{-\lambda_1 x_3} + g_2 B_{12} e^{-\lambda_2 x_3} + g_3 B_{13} e^{-\lambda_3 x_3} + g_4 B_{14} e^{-\lambda_4 x_3}) e^{i\omega t}, \tag{45}$$

$$\widehat{\sigma}_{33} = -\frac{F_1 \widehat{\psi}_1(\xi)}{\Delta} \left(B_{11} \left(\frac{c_{13}}{\rho c_1^2} i\xi - d_1 \lambda_1 \frac{c_{33}}{\rho c_1^2} - p_5 g_1 \right) e^{-\lambda_1 x_3} + B_{12} \left(\frac{c_{13}}{\rho c_1^2} i\xi - d_2 \lambda_2 \frac{c_{33}}{\rho c_1^2} - p_5 g_2 \right) e^{-\lambda_2 x_3} + B_{13} \left(\frac{c_{13}}{\rho c_1^2} i\xi - d_3 \lambda_3 \frac{c_{33}}{\rho c_1^2} - p_5 g_3 \right) e^{-\lambda_3 x_3} + B_{14} \left(\frac{c_{13}}{\rho c_1^2} i\xi - d_4 \lambda_4 \frac{c_{33}}{\rho c_1^2} - p_5 g_4 \right) e^{-\lambda_4 x_3} \right) e^{i\omega t}, \tag{46}$$

$$\widehat{\sigma}_{31} = -\frac{F_1 \widehat{\psi}_1(\xi)}{\rho c_1^2 \Delta} \left(\left(c_{44}(-\lambda_1 + i\xi d_1) + \frac{1}{4l^2} ((l_1^2 G_1 - l_2^2 G_2)(-\xi^2 \lambda_1 - i\xi^3 d_1) + (l_3^2 G_3 - l_2^2 G_2)(\lambda_1^3 + i\xi \lambda_1^2 d_1)) \right) B_{11} e^{-\lambda_1 x_3} + \left(c_{44}(-\lambda_2 + i\xi d_2) + \frac{1}{4l^2} ((l_1^2 G_1 - l_2^2 G_2)(-\xi^2 \lambda_2 - i\xi^3 d_2) + (l_3^2 G_3 - l_2^2 G_2)(\lambda_2^3 + i\xi \lambda_2^2 d_2)) \right) B_{12} e^{-\lambda_2 x_3} + \left(c_{44}(-\lambda_3 + i\xi d_3) + \frac{1}{4l^2} ((l_1^2 G_1 - l_2^2 G_2)(-\xi^2 \lambda_3 - i\xi^3 d_3) + (l_3^2 G_3 - l_2^2 G_2)(\lambda_3^3 + i\xi \lambda_3^2 d_3)) \right) B_{13} e^{-\lambda_3 x_3} + \left(c_{44}(-\lambda_4 + i\xi d_4) + \frac{1}{4l^2} ((l_1^2 G_1 - l_2^2 G_2)(-\xi^2 \lambda_4 - i\xi^3 d_4) + (l_3^2 G_3 - l_2^2 G_2)(\lambda_4^3 + i\xi \lambda_4^2 d_4)) \right) B_{14} e^{-\lambda_4 x_3} \right) e^{i\omega t}, \tag{47}$$

$$\widehat{m}_{32} = -\frac{1}{2} \frac{F_1 \widehat{\psi}_1(\xi)}{\rho c_1^2 l^2 \Delta} (l_2^2 G_2 - l_3^2 G_3) \left(B_{11} e^{-\lambda_1 x_3} (\lambda_1^2 + i\xi \lambda_1 d_1) + B_{12} e^{-\lambda_2 x_3} (\lambda_2^2 + i\xi \lambda_2 d_2) + B_{13} e^{-\lambda_3 x_3} (\lambda_3^2 + i\xi \lambda_3 d_3) + B_{14} e^{-\lambda_4 x_3} (\lambda_4^2 + i\xi \lambda_4 d_4) \right) e^{i\omega t}. \tag{48}$$

where

$$A_{1j} = \left(\frac{i\xi c_{13}}{\rho c_1^2} - \frac{c_{33} \lambda_j d_j}{\rho c_1^2} - p_5 g_j \right),$$

$$A_{2j} = \left(c_{44}(-\lambda_j \frac{1}{\rho c_1^2} + i\xi d_j \frac{1}{\rho c_1^2}) + \frac{1}{4\rho c_1^2 l^2} ((l_1^2 G_1 - l_2^2 G_2)(-\xi^2 \lambda_j - i\xi^3 d_j) + (l_3^2 G_3 - l_2^2 G_2)(-\lambda_j^3 + i\xi \lambda_j^2 d_j)) \right),$$

$$A_{3j} = \frac{1}{2\rho c_1^2 l^2} (l_2^2 G_2 - l_3^2 G_3)(\lambda_j^2 + i\xi \lambda_j d_j),$$

$$A_{4j} = -\lambda_j g_j,$$

$$A_j = -\frac{1}{\Delta} B_{1j} F_1 \widehat{\psi}_1(\xi), \quad j = 1, 2, 3, 4$$

$$\Delta = \Delta_1 - \Delta_2 + \Delta_3 - \Delta_4,$$

$$\Delta_1 = A_{11} A_{22} (A_{33} A_{44} - A_{43} A_{34}) - A_{11} A_{23} (A_{32} A_{44} - A_{42} A_{34}) + A_{11} A_{24} (A_{32} A_{43} - A_{42} A_{33}),$$

$$\Delta_2 = A_{12} A_{21} (A_{33} A_{44} - A_{43} A_{34}) - A_{12} A_{23} (A_{31} A_{44} - A_{41} A_{34}) + A_{24} A_{12} (A_{31} A_{43} - A_{41} A_{33}),$$

$$\Delta_3 = A_{13} A_{21} (A_{32} A_{44} - A_{42} A_{34}) - A_{22} A_{13} (A_{31} A_{44} - A_{41} A_{34}) + A_{13} A_{24} (A_{31} A_{42} - A_{41} A_{32}),$$

$$\Delta_4 = A_{14} A_{21} (A_{32} A_{43} - A_{42} A_{33}) - A_{22} A_{14} (A_{31} A_{43} - A_{41} A_{33}) + A_{14} A_{23} (A_{31} A_{42} - A_{41} A_{32}),$$

$$B_{11} = \Delta_1 / A_{11},$$

$$B_{12} = -\Delta_2 / A_{12},$$

$$B_{13} = \Delta_3 / A_{13},$$

$$B_{14} = -\Delta_4 / A_{14}.$$

Subcase 2(a). Thermal source on the surface of half space

Substituting the values of $\widehat{u}_1, \widehat{u}_3, \widehat{T}$ from Eqs. (32)-(34) in the boundary conditions(39)-(42) and with the aid of (1), (5)-(8),(22)-(23),(27)-(30), we obtain the components of displacement, normal stress, tangential stress, tangential couple stress and temperature change as above with $B_{11}, B_{12}, B_{13}, B_{14}$ replaced by $B_{41}, B_{42}, B_{43}, B_{44}$ and F_1 replaced with $-F_2$.

$$B_{41} = -A_{12} (A_{23} A_{34} - A_{33} A_{24}) + A_{13} (A_{22} A_{34} - A_{32} A_{24}) - A_{14} (A_{22} A_{33} - A_{32} A_{23}),$$

$$B_{41} = -A_{12} (A_{23} A_{34} - A_{33} A_{24}) + A_{13} (A_{22} A_{34} - A_{32} A_{24}) - A_{14} (A_{22} A_{33} - A_{32} A_{23}),$$

$$B_{43} = -A_{11} (A_{22} A_{34} - A_{33} A_{24}) + A_{12} (A_{21} A_{34} - A_{31} A_{24}) - A_{14} (A_{21} A_{32} - A_{31} A_{22}),$$

$$B_{44} = A_{11} (A_{22} A_{33} - A_{23} A_{32}) - A_{12} (A_{21} A_{33} - A_{31} A_{22}) + A_{13} (A_{21} A_{32} - A_{31} A_{22}).$$

4.1 Applications

a) Green's function

To synthesize the Green's function, i.e., the solution due to concentrated normal force and thermal source on the half-space is obtained by setting

$$\psi_1(x) = \delta(x) \tag{49}$$

In Eqs. (43)-(48).Applying the Fourier transform defined by (30) on the Eq. (49) gives

$$\widehat{\psi}_1(\xi) = 1 \tag{50}$$

b) Linearly distributed force

The solution due to distributed force/source applied on the half space is obtained by setting

$$\psi_1(x) = \begin{cases} 1 - \frac{|x|}{m} & \text{if } |x| \leq m \\ 0 & \text{if } |x| > m \end{cases} \tag{51}$$

Here $2m$ is the width of the strip load, the Fourier transformation of (48) in the dimensionless form after suppressing the prime becomes

$$\widehat{\psi}_1(\xi) = [2(1 - \cos(\xi m)) / \xi^2 m], \quad \xi \neq 0. \tag{52}$$

Using (52) in the (43)-(48), we obtain the components of displacement, stresses, temperature change and couple stress.

5. Inversion of the transformations

To obtain the solution of the problem in physical domain, we must invert the transforms in Eqs. (43)-(48). Here the displacement components, normal and tangential stresses and temperature change, couple stress are functions of x_3 , the parameter of Fourier transforms is ξ and hence are of the form $f(\xi, x_3)$. To obtain the function $f(x, x_3)$ in the physical domain, we first invert the Fourier transform using

$$f(x, x_3) = \frac{1}{2\pi} \int_{-\infty}^{\infty} e^{-i\xi x_1} \hat{f}(\xi, x_3) d\xi = \frac{1}{2\pi} \int_{-\infty}^{\infty} |\cos(\xi x)| f_e - i \sin(\xi x) f_0 d\xi. \tag{53}$$

where f_e and f_0 are respectively the odd and even parts of $\hat{f}(\xi, x_3)$. The last step is to calculate the integral in Eq. (55). The method for evaluating this integral is described in Press *et al.* (1986). It involves the use of Romberg's integration with adaptive step size. This also uses the results from successive refinements of the extended trapezoidal rule followed by extrapolation of the results to the limit when the step size tends to zero.

6. Results and discussion

For numerical computations, we take the copper material which is transversely isotropic

$$c_{11} = 18.78 \times 10^{10} \text{ Kgm}^{-1}\text{s}^{-2}, c_{12} = 8.76 \times 10^{10} \text{ Kgm}^{-1}\text{s}^{-2}, c_{13} = 8.0 \times 10^{10} \text{ Kgm}^{-1}\text{s}^{-2}$$

$$c_{33} = 17.2 \times 10^{10} \text{ Kgm}^{-1}\text{s}^{-2}, c_{44} = 5.06 \times 10^{10} \text{ Kgm}^{-1}\text{s}^{-2}, C_E = 0.6331 \times 10^3 \text{ JKg}^{-1}\text{K}^{-1}$$

$$\alpha_1 = 2.98 \times 10^{-5} \text{ K}^{-1}, \alpha_3 = 2.4 \times 10^{-5} \text{ K}^{-1}, T_0 = 293\text{K}, \rho = 8.954 \times 10^3 \text{ Kgm}^{-3}$$

$$K_1 = 0.433 \times 10^3 \text{ Wm}^{-1}\text{K}^{-1}, K_3 = 0.450 \times 10^3 \text{ Wm}^{-1}\text{K}^{-1}, G_1 = 0.1, G_2 = 0.2$$

$$G_3 = 0.3, L = 1, l_1 = l_2 = l_3 = .843$$

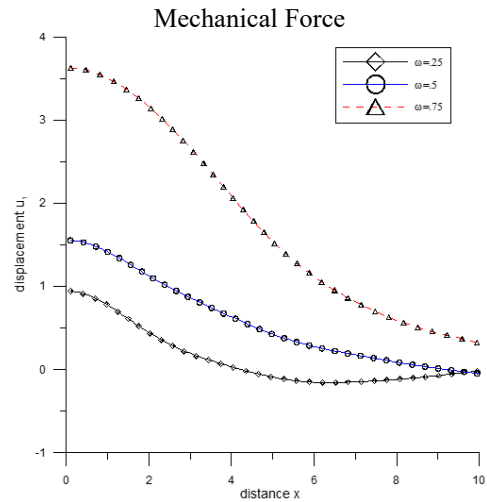


Fig. 1 Variation of displacement u_1 with the distance x (linearly distributed force)

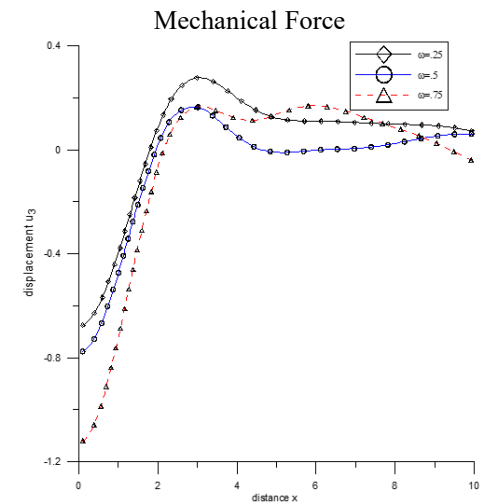


Fig. 2 Variation of displacement u_3 with the distance x (linearly distributed force)

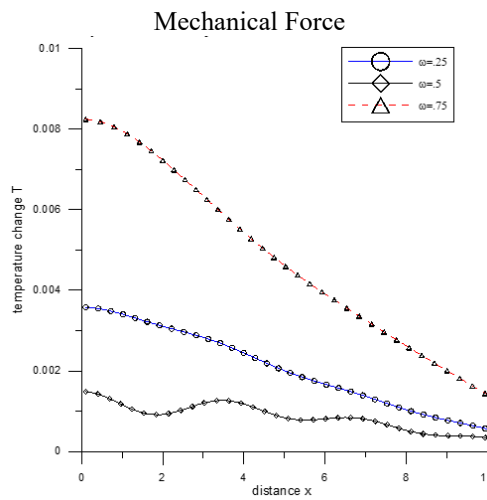


Fig. 3 Variation of temperature change T with the distance x (linearly distributed force)

Components of displacement, stress, temperature change and couple stress are computed numerically. Software GNU

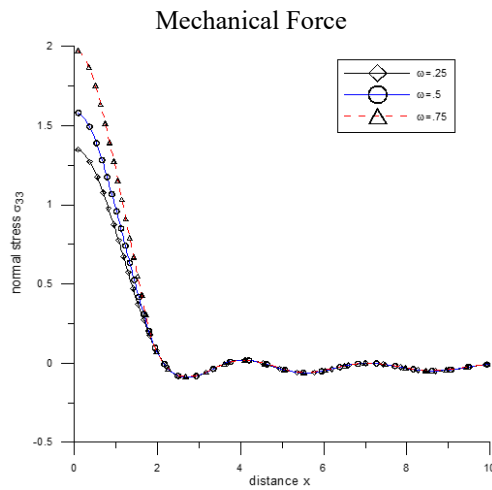


Fig. 4 Variation of normal stress σ_{33} with the distance x (linearly distributed force)

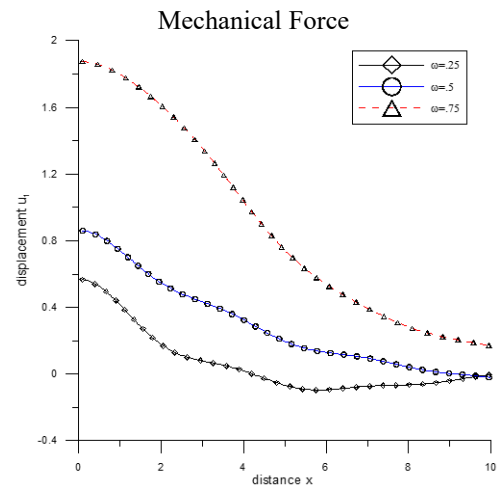


Fig. 7 Variation of displacement u_1 with the distance x (concentrated force)

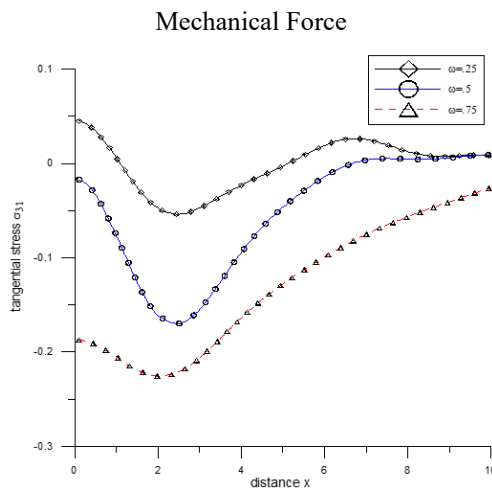


Fig. 5 Variation of tangential stress σ_{31} with the distance x (linearly distributed force)

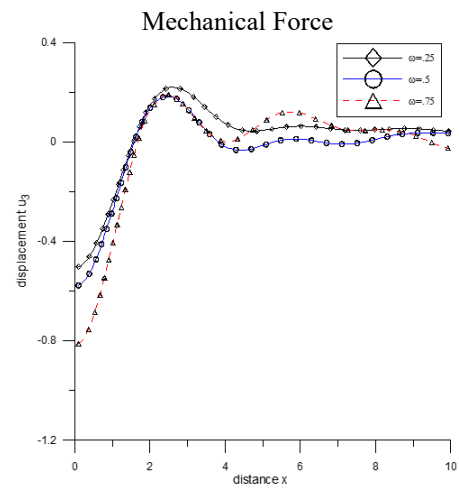


Fig. 8 Variation of displacement u_3 with the distance x (concentrated force)

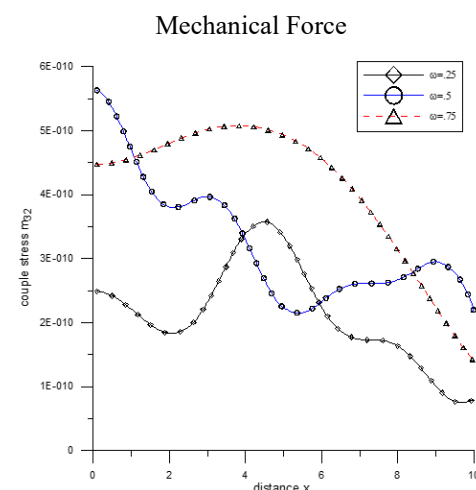


Fig. 6 Variation of couple stress m_{32} with the distance x (linearly distributed force)

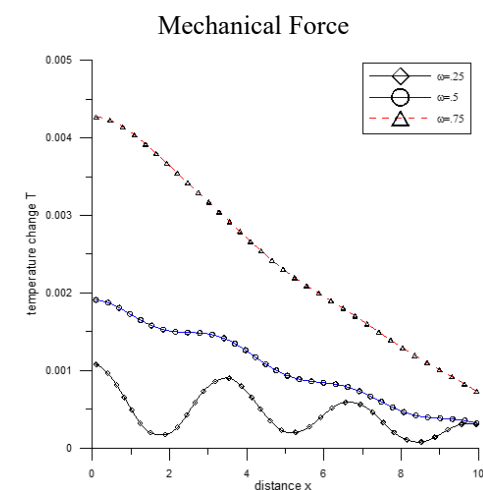


Fig. 9 Variation of temperature change T with the distance x (concentrated force)

Octave 5.1.0 has been used to determine and compare the values of normal stress, tangential stress, couple stress, temperature change and components of displacement for

transversely isotropic thermoelastic medium with distance x for three different values of angular frequency ω . In Figs. 1-36, solid line with centre symbol ($-\diamond$

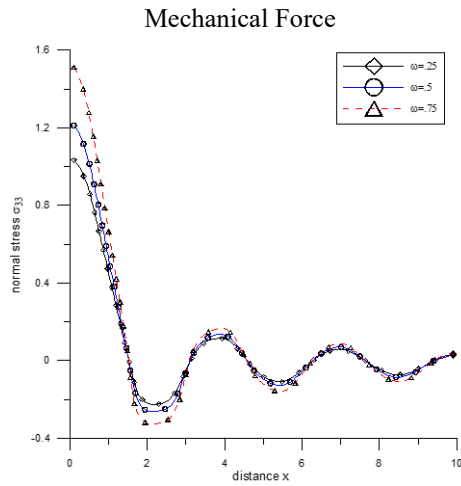


Fig. 10 Variation of normal stress σ_{33} with the distance x (concentrated force)

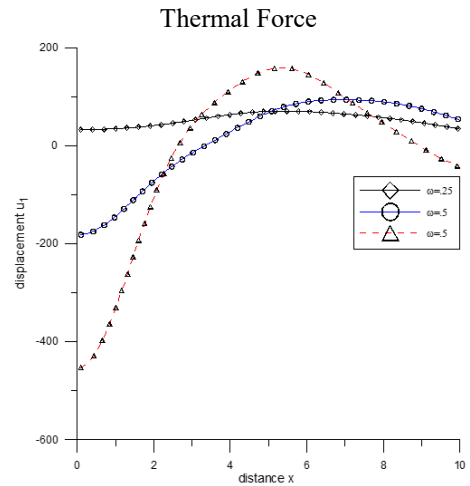


Fig. 13 Variation of displacement u_1 with the distance x (linearly distributed thermal source)

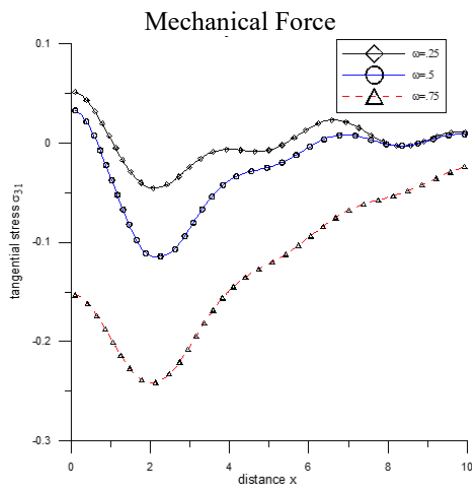


Fig. 11 Variation of tangential stress σ_{31} with the distance x (concentrated force)

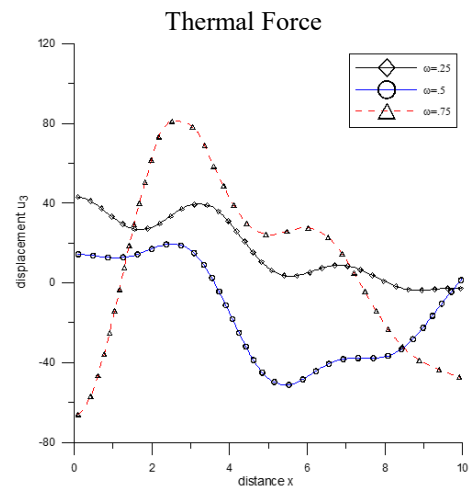


Fig. 14 Variation of displacement u_3 with the distance x (linearly distributed thermal source)

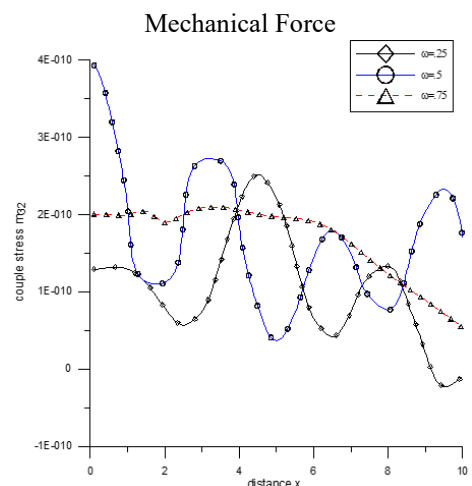


Fig. 12 Variation of couple stress m_{32} with the distance x (concentrated force)

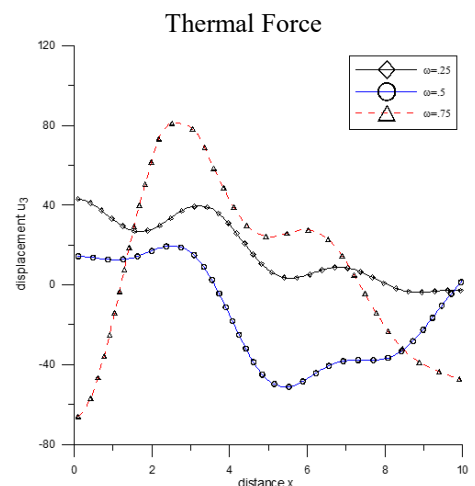


Fig. 15 Variation of displacement u_3 with the distance x (linearly distributed thermal source)

—) corresponds to angular frequency $\omega = .25$ and solid line with centre symbol (— o —) corresponds to angular frequency $\omega = .5$ and dotted line with central symbol

(— Δ —) corresponds to angular frequency $\omega = .75$.

6.1 Mechanical source on the surface of half space

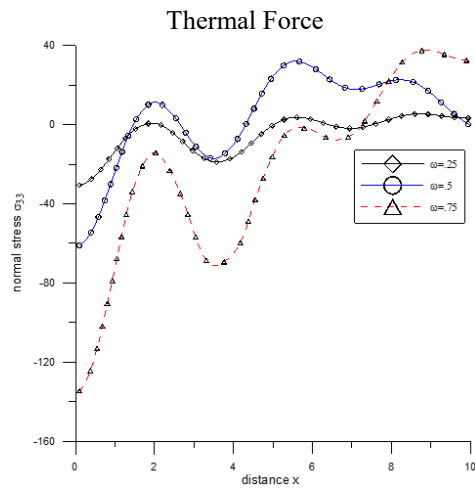


Fig. 16 Variation of normal stress σ_{33} with the distance x (linearly distributed thermal source)

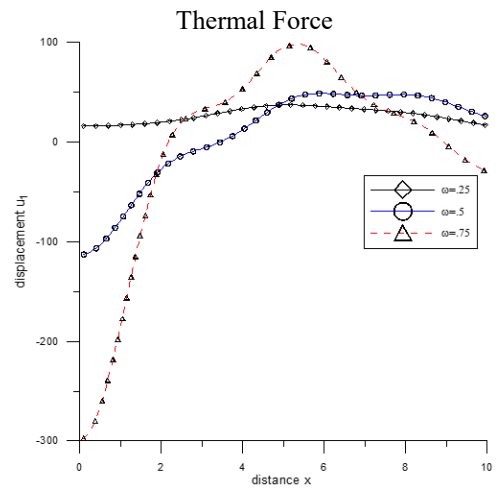


Fig. 19 Variation of displacement u_1 with the distance x (concentrated thermal source)

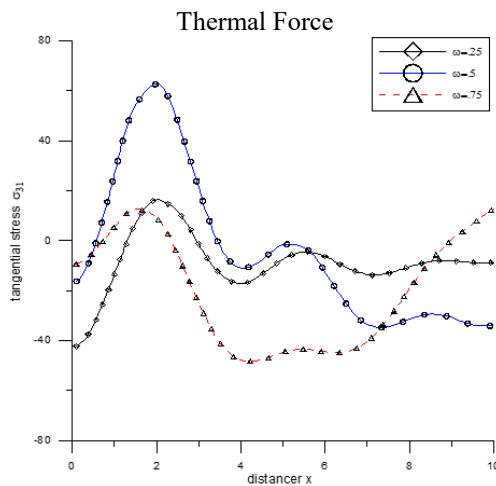


Fig. 17 Variation of tangential stress σ_{31} with the distance x (linearly distributed thermal source)

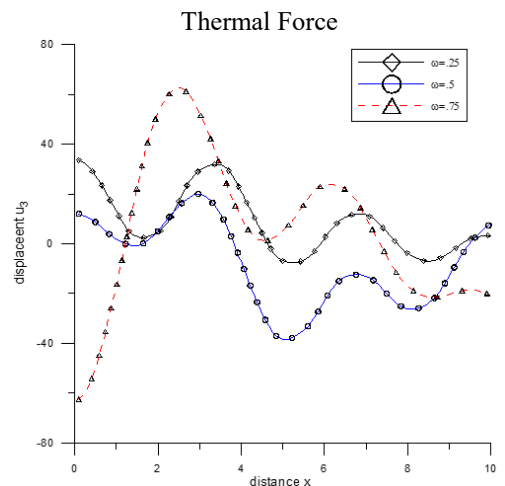


Fig. 20 Variation of displacement u_3 with the distance x (concentrated thermal source)

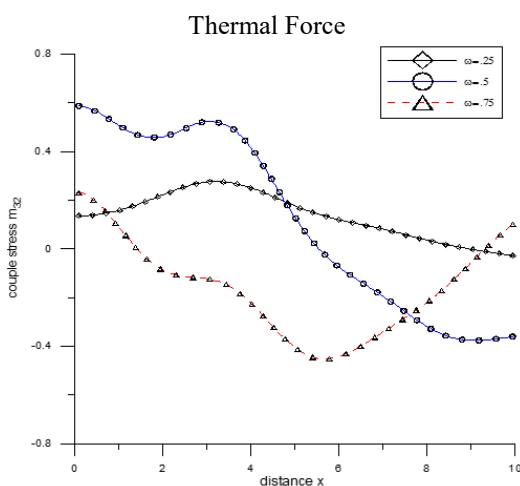


Fig. 18 Variation of couple stress m_{32} with the distance x (linearly distributed thermal source)

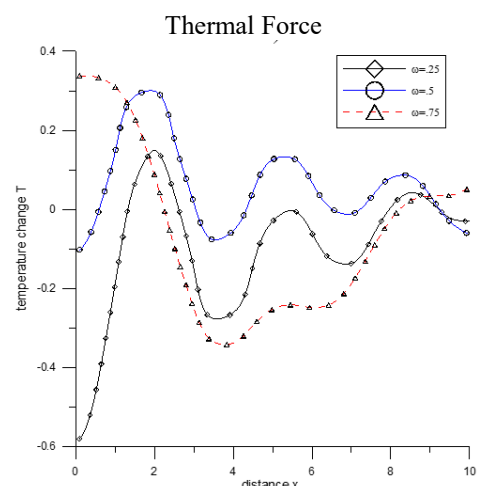


Fig. 21 Variation of temperature change T with the distance x (concentrated thermal source)

a) Linearly distributed mechanical source

Fig.1 shows the variations of the displacement u_1 , for $\omega = .25$ displacement u_1 decreases for $0 \leq x \leq 6.5$ and

rises slowly for the rest of range of x . For $\omega = .5$ and $\omega = .75$ values of u_1 decrease smoothly for $0 \leq x \leq 10$. As x remains constant, u_1 increases with the increase of

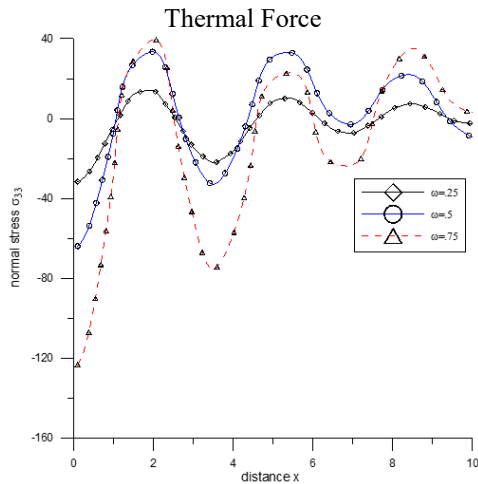


Fig. 22 Variation of normal stress σ_{33} with the distance x (concentrated thermal source)

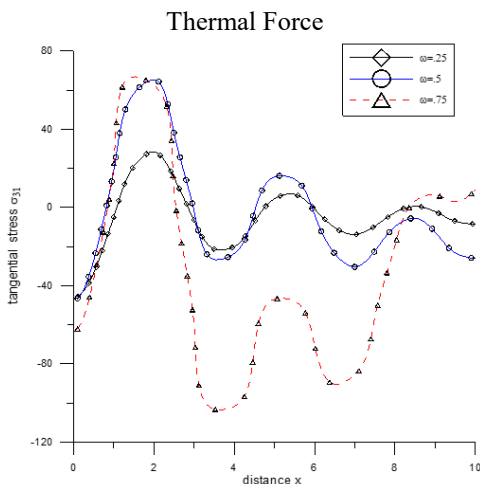


Fig. 23 Variation of tangential stress σ_{31} with the distance x (concentrated thermal source)

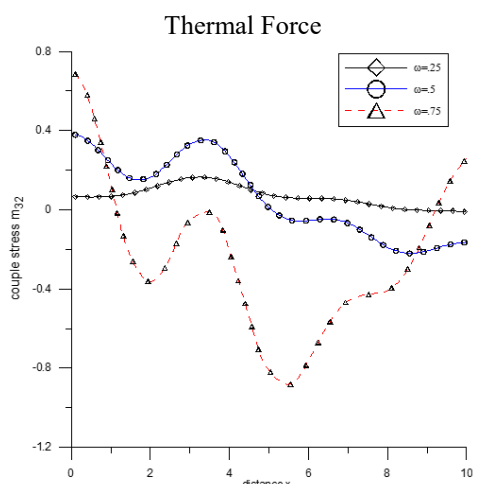


Fig. 24 Variation of couple stress m_{32} with the distance x (concentrated thermal source)

frequency. Fig. 2 shows the variations of the displacement u_3 , for $\omega = .25$ and $\omega = .5$ displacement u_3 monotonically increases for $0 \leq x \leq 4$ and decreases for

$4 \leq x \leq 6$ and increases slowly for the remaining range of x . For $\omega = .75$ trend is similar upto $0 \leq x \leq 6$ and value of u_3 increases for $6 \leq x \leq 7$, then decreases in the rest. Value of u_3 for $\omega = .25$ is higher than that of $\omega = .5$. Fig.3 shows the variations of the temperature change T , for $\omega = .25$ curve shows the oscillatory behavior with small amplitude. For $\omega = .5$ and $\omega = .75$, the value of T shows decreases for the increase in x and increases as frequency ω increases. Fig.4 shows the variations of the normal stress σ_{33} with the distance x . In all the cases i.e., $\omega = .25$, $\omega = .5$ and $\omega = .75$, σ_{33} shows oscillatory behaviour with almost merging small amplitudes for the $4 \leq x \leq 10$ and with a difference in amplitudes in the remaining range. Amplitudes are very high at origin. Fig.5 shows the variations of the tangential stress σ_{31} with the distance x , curves corresponding to frequencies $\omega = .25$, $\omega = .5$ and $\omega = .75$ decrease for $0 \leq x \leq 3$ and increase in the range $3 \leq x \leq 10$. The magnitudes of displacements u_1, u_3 , normal stress are higher near the loading surface than the remaining range. Fig.6 shows the variations of the couple stress m_{32} , curves corresponding to $\omega = .25$ and $\omega = .5$ show oscillatory behavior, curve corresponding to $\omega = .75$ smoothly and monotonically increases in $0 \leq x \leq 5$ and monotonically decreases in the rest of the range.

b) Concentrated mechanical source

Figs. 7-12 show the characteristics for concentrated mechanical source. It is depicted from Figs.7-12 that the distribution curves for u_1, u_3 , normal stress σ_{33} , tangential stress σ_{31} , temperature change T and couple stress m_{32} for concentrated force, follow same trends as in case of linearly distributed force with difference in magnitudes in their respective patterns for all the cases $\omega = .25$, $\omega = .5$ and $\omega = .75$.

6.2 Thermal source on the surface of half space

a) Linearly distributed thermal source

Fig.13 shows the variations of the displacement u_1 , all the three curves increase in the first half and decrease in the rest of the range. Amplitudes are higher for higher values of ω . Fig.14 shows the variations of the displacement u_3 , curve corresponding to $\omega = .25$ increases for $0 \leq x \leq 2$, and then follow descending oscillatory behavior in the rest. Curve corresponding to $\omega = .5$ increases for $0 \leq x \leq 2$, decreases sharply for $2 \leq x \leq 6.5$, increases rapidly in the rest of distance axes. Curve corresponding to $\omega = .75$ increases smoothly for $0 \leq x \leq 4$ and decreases in the rest. Curves do not follow any specific pattern for different frequencies, but very close to the origin as ω increases value of u_3 decreases. Fig.15 shows the variations of the temperature change T , curve corresponding to $\omega = .25$ is ascending oscillatory and curve corresponding to $\omega = .5$ is descending oscillatory. The amplitude of the curves are small. Frequency $\omega = .75$ leads to asymmetrical curve, curve decreases for $0 \leq x \leq 5$ and increases in the rest. Also, amplitude is very large as compare to other two curves. Very near the loading surface, for the higher frequencies, value of T is also higher. Fig.16 shows the variations of the normal stress σ_{33} , curves corresponding to $\omega = .25$, $\omega = .5$ and $\omega = .75$ follow

ascending oscillatory behavior with difference in the magnitude of σ_{33} . Corresponding amplitudes increase as ω increases. At origin, higher frequency curves have lower initial point on σ_{33} axis. Fig.17 shows the variation of tangential stress σ_{31} , curves corresponding to $\omega = .25$ and $\omega = .5$ follow oscillatory behavior with gradually decreasing amplitude. Curve corresponding to $\omega = .5$ follows descending oscillatory behavior. Curve corresponding to $\omega = .75$ decreases for $0 \leq x \leq 5$ and increases in the rest of the range. Fig. 18 shows the variation of the couple stress m_{32} , curves corresponding to all the three frequencies are oscillatory. Value of m_{32} , corresponding to curve $\omega = .75$ is less than both the remaining curves in the range $2 \leq x \leq 8.5$. Value of m_{32} corresponding to $\omega = .25$ and $\omega = .5$ lies in the range $(-0.5, 0.45)$ and corresponding to $\omega = .75$ lies in the range $(-0.4, 0.1)$. Difference among the amplitudes is more in case of tangential stress.

b) Concentrated thermal source

In Fig. 19 distribution curves for u_1 for concentrated thermal force are same as in case of linearly distributed mechanical force except that curves are piecewise smooth. Fig. 20 shows the variations of the displacement u_3 , all the curves are smooth with descending oscillatory behavior. Frequency $\omega = .75$ lead to asymmetry in the pattern of curves. Value of u_3 corresponding to frequencies $\omega = .25$ and $\omega = .5$ monotonically decreases for $0 \leq x \leq 2$, $3.5 \leq x \leq 5$, $7 \leq x \leq 8.5$, and monotonically increases in the rest. Curve corresponding to frequency $\omega = .75$ increase for $0 \leq x \leq 3$, $5 \leq x \leq 6.5$, $9 \leq x \leq 10$, maximum amplitude is in the range $1.5 \leq x \leq 4$. Except for curve corresponding to $\omega = .5$, amplitude of curves decrease as we move toward right along the distance axis. Fig.21 shows the variations of the temperature T , curves are smooth with oscillatory behavior. Frequency $\omega = .75$ leads to some asymmetry in the shape of curves. Corresponding amplitudes decrease as ω increases. Curve corresponding to frequency $\omega = .75$ decreases for $0 \leq x \leq 4$, is ascending oscillatory in rest. Fig.22 shows the variations of the normal stress σ_{33} , all the curves are smooth with oscillatory behavior. Corresponding amplitudes increase as frequency increases. Fig.23 shows the variations of the tangential stress σ_{31} , curves are smooth oscillatory with alternatively monotonically increasing and decreasing behavior. Amplitude of variation goes on increase as frequency increases. Increase in frequency lead to asymmetry in the shape of curve. Fig.24 shows the variations of the couple stress m_{32} , curve corresponding to $\omega = .25$ and $\omega = .5$ show oscillatory behavior with higher amplitude of the curve for $\omega = .5$. Curve corresponding to $\omega = .75$ is descending oscillatory in $0 \leq x \leq 5.5$ having large amplitude and is ascending oscillatory in the remaining range having small amplitude.

7. Conclusions

New modified couple stress theory for transverse isotropic thermoelastic medium in frequency domain is presented in this paper. Size effects are considered using

length scale parameters. Analysis of stresses, temperature change, displacement components and couple stress due to thermal and mechanical changes in transversely isotropic material is a significant problem in solid mechanics. The interactions of a transversely isotropic thermoelastic material in the new modified couple stress theory have been investigated using harmonic behavior and Fourier transform technique. A numerical inversion technique has been used to recover the solutions in the physical domain. The expressions for components of stress, components of displacement, temperature change and couple stress have been derived successfully and shown graphically in the presence of angular frequency. All the analysis has been done varying the angular frequency ω . Figures show that the angular frequency has appreciable effects on the numerical values of the resulting quantities. The results obtained in the study should be beneficial for people working on new modified couple stress thermoelastic solid without energy dissipation and similar work.

Acknowledgments

The corresponding author Harpreet Kaur duly acknowledges the Junior Research Fellowship(JRF) received from University Grants Commission (UGC), Delhi India for pursuing her Ph.D. under the sanctioned no. 19/6/2016/(i) EU-V.

References

- Abbas I.A. (2016), "Free vibration of a thermoelastic hollow cylinder under two-temperature generalized thermoelastic theory", *Mech. Based Des. Struct. Machines*, **45**(3), 395-405. <https://doi.org/10.1080/15397734.2016.1231065>.
- Abbas, I.A. (2014), "Three-phase lag model on thermoelastic interaction in an unbounded fiber-reinforced anisotropic medium with a cylindrical cavity", *J. Comput. Theor. Nanosci.*, **11**(4), 987-992. <https://doi.org/10.1166/jctn.2014.3454>.
- Abbas, I.A. (2014c), "Eigenvalue approach for an unbounded medium with a spherical cavity based upon two-temperature generalized thermoelastic theory", *J. Mech. Sci. Technol.*, **28**(10), 4193-4198. <https://doi.org/10.1007/s12206-014-0932-6>.
- Abbas, I.A. (2015), "A dual phase lag model on thermoelastic interaction in an infinite fiber reinforced anisotropic medium with a circular hole", *Mech. Based Des. Struct. Machines*, **43**(4), 501-513. <https://doi.org/10.1080/15397734.2015.1029589>.
- Abbas, I.A. and Youssef, H.M. (2009), "Finite element analysis of two-temperature generalized magneto-thermoelasticity", *Arch. Appl. Mech.*, **79**, 917-925. <https://doi.org/10.1007/s00419-008-0259-9>.
- Abbas, I.A. and Zenkour, A.M. (2014a), "Two-temperature generalized thermoelastic interaction in an infinite fiber-reinforced anisotropic plate containing a circular cavity with two relaxation times", *J. Comput. Theor. Nanosci.*, **11** (1), 1-7. <https://doi.org/10.1166/jctn.2014.3309>.
- Ansari, R., Ashrafi, M.A. and Hosseinzadeh, S. (2014), "Vibration characteristics of piezoelectric microbeams based on the modified couple stress theory", *Shock Vib.*, **2014**(1), 1-12. <http://dx.doi.org/10.1155/2014/598292>.
- Arif, S.M., Biwi, M. and Jahangir, A. (2018) "Solution of algebraic lyapunov equation on positive-definite hermitian

- matrices by using extended Hamiltonian algorithm”, *Comput. Mater. Continua*, **54**, 181-195.
- Atanasov, M.S., Karličić, D., Kozic, P. and Janevski, G. (2017), “Thermal effect on free vibration and buckling of a double-microbeam system”, *Facta Universitatis Ser. Mech. Eng.*, **15**(1), 45-62. <https://doi.org/10.22190/FUME161115007S>.
- Chen, W. and Li, X. (2014), “A new modified couple stress theory for anisotropic elasticity and microscale laminated Kirchhoff plate model”, *Arch. Appl. Mech.*, **84**(3), 323-341. <https://doi.org/10.1007/s00419-013-0802-1>.
- Chen, W., Yang, S. and Li, X. (2014), “A study of scale effect of composite laminated plates based on new modified couple stress theory by finite-element method”, *J. Multiscale Comput. Eng.*, **12**(6), 507-527. <https://doi.org/10.1615/IntJMultCompEng.2014011286>.
- Cosserrat, E. and Cosserrat, F. (1909), *Theory of Deformable Bodies*, Hermann et Fils, Paris, France.
- Hadjesfandiari, A.R. and Dargush, G.F. (2011), “Couple stress theory for solids”, *Int. J. Solids Struct.*, **48**(18), 2496-2510. <https://doi.org/10.1016/j.ijsolstr.2011.05.002>.
- Hadjesfandiari, A.R., Hadjesfandiari, A., Zhang, H. and Dargush, G.F. (2018), “Size-dependent couple stress Timoshenko beam theory”, *preprint arXiv:1712.08527*.
- Honig, G. and Hirdes, U. (1984), “A method for the numerical inversion of the Laplace transform”, *J. Comput. Appl. Math.*, **10**(1), 113-132. [https://doi.org/10.1016/0377-0427\(84\)90075-X](https://doi.org/10.1016/0377-0427(84)90075-X).
- Kang, X., Yang, F.J. and He, X.Y. (2012), “Nonlinearity analysis of piezoelectric micromachined ultrasonic transducers based on couple stress theory”, *Acta Mechanica Sinica*, **28**(1), 104-111. <https://doi.org/10.1007/s10409-012-0019-5>.
- Kaushal, S., Kumar, R. and Miglani, A. (2010), “Response of frequency domain in generalized thermoelasticity with two temperatures”, *J. Eng. Phys. Thermophys.*, **83**(5), 1080-1088. <https://doi.org/10.1007/s10891-010-0433-0>.
- Ke, L.L., Wang, Y.S., Yang, J. and Kitipornchai, S. (2012), “Nonlinear free vibration of size-dependent functionally graded microbeams”, *Int. J. Eng. Sci.*, **50**(1), 256-267. <https://doi.org/10.1016/j.ijengsci.2010.12.008>.
- Koiter, W.T. (1964), “Couple stresses in the theory of elasticity, I and II”, *Nederl. Akad. Wetensch. Proc. Serial B*, **67**, 17-29.
- Kumar, R. and Devi, S. (2015), “Interaction due to Hall current and rotation in a modified couple stress elastic half-space due to ramp-type loading”, *Comput. Meth. Sci. Technol.*, **21**(4), 229-240. <https://doi.org/10.12921/cmst.2015.21.04.007>.
- Kumar, R., Devi, S. and Sharma, V. (2017), “Deformation due to expanding ring load in modified couple stress thermoelastic diffusion in time and frequency domain”, *Mech. Adv. Mater. Struct.*, **24**(8), 685-697. <https://doi.org/10.1080/15376494.2016.1196775>.
- Kumar, R., Sharma, N. and Lata, P. (2016), “Effects of Hall current and two temperatures in transversely isotropic magneto-thermoelastic with and without energy dissipation due to ramp type heat”, *Mech. Adv. Mater. Struct.*, **24**(8), 625-635. <https://doi.org/10.1080/15376494.2016.1196769>.
- Kumar, R., Sharma, N. and Lata, P. (2016a), “Thermomechanical interactions due to Hall current in transversely isotropic thermoelastic medium with and without energy dissipation with two temperatures and rotation”, *J. Solid Mech.*, **8**(4), 840-858.
- Kumar, R., Sharma, N., Lata, P. and Abo-Dahab, S. M. (2017a), “Mathematical modelling of Stoneley wave in a transversely isotropic thermoelastic media”, *Appl. Appl. Math.*, **12**(1), 319-336.
- Kumar, R., Sharma, N., Lata, P. and Abo-Dahab, S.M. (2017), “Rayleigh waves in anisotropic magneto-thermoelastic medium”, *Coupled Syst. Mech.*, **6**(3), 317-333. <https://doi.org/10.12989/csm.2017.6.3.317>.
- Lata, P. and Kaur, I. (2019), “Transversely isotropic thick plate with two temperature and GN type-III in frequency domain”, *Coupled Syst. Mech.*, **8**(1), 55-70. <http://doi.org/10.12989/csm.2019.8.1.055>.
- Lata, P. and Kaur, I. (2019a), “Thermomechanical Interactions in transversely isotropic thick circular plate with axisymmetric heat supply”, *Struct. Eng. Mech.*, **69**(6), 607-614. <http://doi.org/10.12989/sem.2019.69.6.60>.
- Lata, P. and Kaur, I. (2019b), “Thermomechanical interactions in a transversely isotropic magneto thermoelastic solids with two temperature and rotation due to time harmonic sources”, *Coupled Syst. Mech.*, **8**(3), 219-245. <http://doi.org/10.12989/csm.2019.8.3.219>.
- Li, Y., Meguid, S.A., Fu, Y. and Xu, D. (2013), “Nonlinear analysis of thermally and electrically actuated functionally graded material microbeam”, *Proc. Royal Soc. A Math. Phys. Eng. Sci.*, **470**(2162), 1-17. <https://doi.org/10.1098/rspa.2013.0473>.
- Marin, M. (2007), “Weak solutions in elasticity of dipolar porous materials”, *Math. Prob. Eng.*, **2008**, 1-8. <http://dx.doi.org/10.1155/2008/158908>.
- Marin, M. (1997), “On weak solutions in elasticity of dipolar bodies with voids”, *J. Comput. Appl. Math.*, **82**(1-2), 291-297. [https://doi.org/10.1016/S0377-0427\(97\)00047-2](https://doi.org/10.1016/S0377-0427(97)00047-2).
- Marin, M. (1998), “Contributions on uniqueness in thermoelastodynamics on bodies with voids”, *Revista Ciencias Matematicas (Havana)*, **16**(2), 101-109.
- Marin, M. and Stan, G. (2013), “Weak solutions in elasticity of dipolar bodies with stretch”, *Carpathian J. Math.*, **29**(1), 33-40. <http://dx.doi.org/10.1155/2008/158908>.
- Mindlin, R.D. and Tiersten, H.F. (1962), “Effects of couple-stress in linear elasticity”, *Arch. Rational Mech. Anal.*, **11**(1), 415-448. <https://doi.org/10.1007/BF00253946>.
- Najafi, M., Rezaadeh, G. and Shabani, R. (2012), “Thermo-elastic damping in a capacitive micro-beam resonator considering hyperbolic heat conduction model and modified couple stress theory”, *J. Solid Mech.*, **4**(4), 386-401.
- Othman M.I.A. and Abbas, I.A. (2012), “Generalized thermoelasticity of thermal-shock problem in a nonhomogeneous isotropic hollow cylinder with energy dissipation”, *Int. J. Thermophys.*, **33**(5), 913-923. <https://doi.org/10.1007/s10598-011-9102-1>.
- Othman, M.I.A., Atwa, S.Y., Jahangir, A. and Khan, A. (2013), “Generalized magneto-thermo-microstretch elastic solid under gravitational effect with energy dissipation” *Multidiscipline Model. Mater. Struct.*, **9**(2), 145-176. <https://doi.org/10.1108/MMMS-01-2013-0005>.
- Othman, M.I.A., Atwa, S.Y., Jahangir, A. and Khan, A. (2015), “The effect of gravity on plane waves in a rotating thermo-microstretch elastic solid for a mode-I crack with energy dissipation” *Mech. Adv. Mater. Struct.*, **22**(11), 945-955. <https://doi.org/10.1080/15376494.2014.884657>.
- Othman, M.I.A., Jahangir, A. and Nadia, A. (2018a), “Microstretch thermoelastic solid with temperature-dependent elastic properties under the influence of magnetic and gravitational field”, *J. Brazilian Soc. Mech. Sci. Eng.*, **40**(7), 332. <https://doi.org/10.1007/s40430-018-1204-7>.
- Press, W.H., Teukolsky, S.A., Vetterling, W.T. and Flannery, B.P. (1986), *Numerical Recipe*, Cambridge University Press.
- Roque, C.M.C., Ferreira, A.J.M. and Reddy, J.N. (2013), “Analysis of Mindlin micro plates with a modified couple stress theory and a meshless method”, *Appl. Math. Modell.*, **37**(7), 4626-4633. <https://doi.org/10.1016/j.apm.2012.09.063>.
- Shaat, M., Mahmoud, F.F., Gao, X.L. and Faheem, A.F. (2014), “Size dependent bending analysis of Kirchhoff nano-plates based on a modified couple-stress theory including surface effects”, *Int. J. Mech. Sci.*, **79**, 31-37. <https://doi.org/10.1016/j.ijmecsci.2013.11.022>.

- Sharma, N., Kumar, R. and Lata, P. (2015), "Disturbance due to inclined load in transversely isotropic thermoelastic medium with two temperatures and without energy dissipation", *Mater. Phys. Mech.*, **22**, 107-117.
- Slaughter, W.S. (2002), *The Linearised Theory of Elasticity*, Birkhäuser Boston, Cambridge, Massachusetts, U.S.A.
- Thai, H.T., Vo, T.P., Nguyen, T.K. and Lee, J. (2014), "Size-dependent behavior of functionally graded sandwich microbeams based on the modified couple stress theory", *Compos. Struct.*, **123**, 337-349.
<https://doi.org/10.1016/j.compstruct.2014.11.065>.
- Tiwari, G. (1971), "Effect of couple-stresses in a semi-infinite elastic medium due to impulsive twist over the surface", *Pure Appl. Geophys.*, **91**(1), 71-75.
<https://doi.org/10.1007/BF00877889>.
- Togun, N. and Bağdatlı, S.M. (2017), "Investigation of the size effect in Euler-Bernoulli nanobeam using the modified couple stress theory", *Celal Bayar Univ. J. Sci.*, **13**(4), 893-899.
<https://doi.org/10.18466/cbayarfbe.370362>.
- Usman, M., Saba, K., Jahangir, A., Kamran, M. and Muhammad, N. (2018b), "Electromechanical fields and their influence on the internal quantum efficiency of GaN-based light-emitting diodes", *Acta Mechanica Solida Sinica*, **31**(3), 383-390.
<https://doi.org/10.1007/s10338-018-0013-y>.
- Wang, L., Xu, Y. and Ni, Q. (2013), "Size-dependent vibration analysis of three-dimensional cylindrical microbeams based on modified couple stress theory: A unified treatment", *Int. J. Eng. Sci.*, **68**, 1-10. <https://doi.org/10.1016/j.ijengsci.2013.03.004>.
- Yang, F., Chong, A.C.M., Lam, D.C.C. and Tong, P. (2002), "Couple stress based strain gradient theory for elasticity", *Int. J. Solids Struct.*, **39**(10), 2731-2743.
[https://doi.org/10.1016/S0020-7683\(02\)00152-X](https://doi.org/10.1016/S0020-7683(02)00152-X).
- Zenkour, A.M. (2018), "Modified couple stress theory for micro-machined beam resonators with linearly varying thickness and various boundary conditions", *Arch. Mech. Eng.*, **65**(1), 41-64.
<https://doi.org/10.24425/119409>.
- Zenkour, A.M. and Abbas, I.A. (2014b), "A generalized thermoelasticity problem of an annular cylinder with temperature-dependent density and material properties", *Int. J. Mech. Sci.*, **84**, 54-60.
<https://doi.org/10.1016/j.ijmecsci.2014.03.016>.